Contributions of mature granule cells to structural plasticity in temporal lobe epilepsy

Victor R. Santos[1,5,*], **Olagide Wagner de Castro**[1,5,*], **Raymund Y.K. Pun**[1], **Michael S. Hester**[4], **Brian L. Murphy**[1,3], **Andreas W. Loepke**[1,2,3], **Norberto Garcia-Cairasco**[5], and **Steve C. Danzer**[1,2,3,4]

[1]Department of Anesthesia, Cincinnati Children's Hospital Medical Center, Cincinnati, OH

[2]Department of Anesthesia and Pediatrics, University of Cincinnati, Cincinnati, OH

[3]Program in Neuroscience, University of Cincinnati, Cincinnati, OH

[4]Molecular and Developmental Biology Graduate Program, University of Cincinnati, Cincinnati, Ohio

[5]Department of Physiology, Ribeirão Preto School of Medicine, University of São Paulo, Ribeirão Preto, SP, 14049900

Abstract

During the development of epilepsy in adult animals, newly-generated granule cells integrate abnormally into the hippocampus. These new cells migrate to ectopic locations in the hilus, develop aberrant basal dendrites, contribute to mossy fiber sprouting and exhibit changes in apical dendrite structure and dendritic spine number. Mature granule cells do not appear to exhibit migration defects, basal dendrites and mossy fiber sprouting, but whether they exhibit apical dendrite abnormalities or spine changes is not known. To address these questions, we examined the apical dendritic structure of BrdU-birthdated, GFP-expressing granule cells born two months before pilocarpine-induced status epilepticus. In contrast to immature granule cells, exposing mature granule cells to status epilepticus did not significantly disrupt the branching structure of their apical dendrites. Mature granule cells did, however, exhibit significant reductions in spine density and spine number relative to age-matched cells from control animals. These data demonstrate that while mature granule cells are resistant to developing the gross structural abnormalities exhibited by younger granule cells, they show similar plastic rearrangement of their dendritic spines.

Keywords

adult neurogenesis; basal dendrite; mossy fiber sprouting; dendritic spine; hilar ectopic granule cell; pilocarpine; status epilepticus

Corresponding author: (Laboratory of Origin), Dr. Steve C. Danzer, 3333 Burnet Avenue, ML 2001, Cincinnati, Ohio 45229-3039, (513) 636-4526 (phone), (513) 636-7337 (fax), steve.danzer@cchmc.org.
*These authors contributed equally to this work.

Introduction

Temporal lobe epilepsy is a common and debilitating disease that, in addition to seizures, is sometimes associated with significant cognitive and memory deficits. Recently, attention has focused on the impact of seizures and epileptogenesis on adult neurogenesis. In both animals and humans, hippocampal granule cells are generated throughout life and into old age (Altman and Das, 1965; Kaplan and Hinds, 1977; Eriksson et al., 1998; van Praag et al., 2002). While the exact role of these new cells remains controversial, numerous animal studies have linked them to learning and memory (for review see Deng et al., 2010). During the development of epilepsy, however, newly-generated granule cells integrate abnormally into the brain. Indeed, abnormal, adult-generated granule cells appear to account for much of the pathological plastic rearrangement of the epileptic dentate gyrus. Specifically, new cells appear to underlie mossy fiber sprouting (Parent et al., 1997; Kron et al., 2010), in which granule cells innervate the dentate inner molecular layer, creating recurrent excitatory connections (Nadler, 2003). New cells migrate to ectopic locations in the dentate hilus (Scharfman et al., 2000; Parent et al., 2006), where they exhibit abnormal morphological and physiological properties (Pierce et al., 2005; Cameron et al., 2011; Pierce et al., 2011). New cells form basal dendrites (Walter et al., 2007), which project into the dentate hilus and establish additional recurrent connections with other granule cells (Ribak et al., 2000; Shapiro and Ribak, 2006; Thind et al., 2008), and new cells exhibit a variety of apical dendrite abnormalities (Murphy et al., 2011).

While previous studies indicate that mature granule cells are comparatively resistant to developing the more extravagant plastic changes exhibited by immature cells, such as formation of hilar basal dendrites (Jessberger et al., 2007; Walter et al., 2007), it seems improbable that they are entirely unaffected by the epileptogenic process. Indeed, numerous studies going back decades (here citing just a few examples; Scheibel and Scheibel, 1973, Geinisman et al., 1988; Houser, 1990; Bundman et al., 1994; von Campe et al., 1997; da Silva et al., 2006; Murphy and Danzer, 2011) have identified changes among granule cells during epileptogenesis. Although cell age was not determined in these studies, it is likely that most reflect changes among mature neurons given the relative proportions of mature to immature cells (Mathews et al., 2010). To explore this possibility, granule cells born two months before pilocarpine-induced status epilepticus were examined one month after the injury. A smaller group of cells born one week before status epilepticus (immature cells) was also included for comparative purposes. Cells were birthdated and their morphology revealed by treating GFP-expressing mice with the thymidine analog BrdU (Walter et al., 2007; Murphy et al., 2011). Recent findings have led to the hypothesis that aberrant integration of adult-generated granule cells contributes to the etiology of temporal lobe epilepsy (Parent and Murphy, 2008). Despite the heightened role of these immature cells, it is still important to elucidate whether and how their more mature neighbors respond to the insult.

Experimental procedures

BrdU neuronal birthdating and pilocarpine epileptogenesis

All procedures conformed to NIH and institutional guidelines for the care and use of animals. Studies were conducted on Thy1-GFP expressing mice maintained on a C57BL/6 background (Feng et al., 2000). Mice were hemizygous (carried one copy) for the Thy1-GFP transgene. Although multiple litters were used to generate sufficient animals for study, littermates were represented in both control and experimental groups to reduce variability.

To examine the impact of status epilepticus (SE) on mature cells, 12 one-month-old male mice (control, n=7; SE, n=5) were given once-daily subcutaneous (s.c.) injections of BrdU

(100 mg/kg in Ringers solution) for three days. Two months later, mice were injected with 1mg/kg methyl scopolamine nitrate s.c. followed by 380 mg/kg pilocarpine. Injections were given between 10AM and noon to control for diurnal variations. The development of status epilepticus in pilocarpine-treated mice was confirmed by behavioral observation. Three hours after the onset of status epilepticus, mice were given two doses of 10 mg/kg diazepam at 15 minute intervals. Control animals received saline instead of pilocarpine, but were given all other drugs and treatments. Four weeks after pilocarpine treatment, mice were anesthetized with pentobarbital (100 mg/kg) and perfused with PBS+1U/ml heparin followed by 2.5% paraformaldehyde and 4% sucrose in PBS, pH 7.4. Brains were post-fixed overnight, cryoprotected in sucrose (10, 20, 30%), and sectioned coronally at 60 μm. Slide-mounted sections were stored at −80°C. Cells generated using this protocol are designated as "mature/no SE" or "mature+SE", depending on whether the animals received saline or pilocarpine-status epilepticus, respectively.

For comparative purposes, thirteen male mice were injected with BrdU beginning one week prior to pilocarpine treatment and were perfusion fixed four weeks after treatment. Mice were either one- or three-months-old at the time of pilocarpine-treatment (control, 1 month, n=3; control, 3 months, n=3; SE, 1 month, n=4; SE, 3 months, n=3). One-month-old animals were included in an attempt to increase the yield of immature/no SE cells, since constitutive neurogenesis is higher in young animals. Yields were low because the Thy1 promoter does not begin to drive GFP expression until the cells are ≈4 weeks old, and many cells were too faint for reliable reconstruction at the five week time point. Treatments to increase neurogenesis (e.g., wheel running) would improve yields, but also introduce potentially confounding variables (Arida et al., 1998), so animals were housed under standard conditions. Cells generated using this protocol were five weeks old at the time of perfusion, and are designated as "immature/no SE" or "immature+SE", depending on whether the animals received saline or pilocarpine-status epilepticus, respectively. All other treatments were identical to those described for examining mature granule cells.

Immunohistochemistry

Immunohistochemistry was conducted for BrdU and GFP in accord with established protocols (Murphy et al., 2011). Briefly, slide-mounted brain sections were incubated overnight at 4°C in 1:200 mouse monoclonal anti-BrdU antibodies (Becton, Dickinson and Company, Franklin Lakes, NJ) and 5 μg/ml rabbit polyclonal anti-GFP (AB3080, Chemicon, Temecula, CA) or 1:1500 chicken anti-GFP (#AB13970, Abcam) antibodies. Alexa Fluor 594 goat anti-mouse, Alexa Fluor 488 goat anti-rabbit and Alexa Fluor 488 goat anti-chicken secondary antibodies were used, as appropriate, at a 1:750 dilution (Molecular Probes, Eugene, OR).

Confocal microscopy

Neuronal selection and reconstruction were conducted with the investigator blinded to treatment group. BrdU-positive, GFP-expressing dentate granule cells were identified by screening immunostained sections under epifluorescent illumination. All double-labeled cells meeting the following criteria were selected for analysis:

1. Soma contained within the tissue section, such that the number of apical and basal processes could be accurately determined.

2. At least one apical dendrite branch terminating naturally (not artificially truncated at the tissue surface).

3. Bright GFP-labeling to ensure accurate reconstruction.

Cells meeting these criteria were imaged using a Leica SP5 confocal system set up on a DMI6000 inverted microscope equipped with a 63× oil immersion objective (NA 1.4). For dendritic reconstructions, 3-dimensional Z-series stacks were captured at 0.5 μm increments with a resolution of 0.12μm/pixel.

Neuronal Reconstructions

Neurons were digitally reconstructed from confocal image stacks using Neurolucida software (Microbrightfield, Inc.). Dendritic endings were encoded either as "natural" if they ended normally within the tissue section, or "truncated" if they were cut at either the upper or lower surface of the tissue slice. The position of each cell within the upper or lower blade of the dentate, and cell position relative to the hilar border and relative to bregma coordinates (Paxinos and Franklin, 2001) was recorded. The number of truncated endings and cell position were statistically equivalent among groups (data not shown). Image stacks were also used to encode the location of the hilar – granule cell body layer border, the granule cell body layer – molecular layer border and the location of the hippocampal fissure. The molecular layer was further subdivided into inner, middle and outer regions, with the inner region being the first 17% of the molecular layer (West and Andersen, 1980; Deller et al., 1999; van Groen et al., 2003; Danzer et al., 2004; Murphy et al., 2011), and the middle and outer being an equal split of the remainder. These subdivisions are only approximate, however, because exact divisions between layers are not clearly discernable.

Spine Counts

Dendritic spines were counted from 3-dimensional z-series confocal image stacks using Neurolucida software. Z-series stacks were captured at 0.2 μm increments with a 63× (1.4 NA) objective at 6× optical zoom. Stacks were obtained from the inner, middle and outer molecular layers, corresponding to the three distinct lamina of the dentate molecular layer. Only dendritic segments fully contained within the tissue section were imaged for spine count analysis. Spines were defined as protrusions from the dendritic shaft exceeding 0.25 μm in length. Confocal z-series stacks facilitate the visualization of spines above and below the dendrite, as well as spines along the sides of the dendrite. Spines above and below the dendrite still tend to be somewhat obscured, however, so counts presented here may underestimate actual spine numbers.

Statistics

Statistical tests were conducted using Sigma Plot software (version 11.0). For comparisons of mature/no SE and mature+SE groups, which consisted entirely of animals treated with pilocarpine at three months of age, data were assessed for normality and equal variance, and parametric or non-parametric tests were run as appropriate. Actual tests used are noted in the results. For comparisons of immature/no SE and immature+SE groups, which contained animals that received pilocarpine (or saline) at either one or three months of age, data were assessed for normality and equal variance, and were normalized using a rank transformation if necessary. Significance was then determined used a two-way ANOVA controlling for age and treatment with a Holm-Sidak post-test. P values < α=0.05 were accepted as significant.

Figure preparation

Confocal maximum projections were generated from z-series stacks using Leica's LAS-AF Confocal Application Suite (version 2.2.0 build 4758). Images were processed using an erosion filter run for one iteration with a three pixel radius to reduce background artifact. Z-series stacks were also cropped in the z-dimension to remove structures of other neurons that would otherwise obscure the cell of interest in two dimensional projections (Walter et al., 2007). Final figure preparation, including adjustments of brightness and contrast, was done

using Photoshop software (version 7.0). Identical adjustments were made to images meant for comparison.

Results

To assess the impact of status epilepticus (SE) on the structure of mature granule cells, Thy1-GFP expressing mice were treated with BrdU to label adult-generated granule cells, and were subsequently treated with pilocarpine to induce SE. Sections from these animals were screened to identify BrdU-labeled, GFP-expressing cells for analysis, with the co-incidence of both labels revealing cell age and morphology (Fig.1). Four groups of BrdU-labeled, GFP-expressing adult-generated cells were examined: 1) Mature/no SE: BrdU-labeled, GFP expressing cells from animals treated with BrdU twelve weeks earlier (n=18 cells). 2) Mature+SE: Cells from animals treated with BrdU eight weeks before pilocarpine SE, and killed four weeks after SE (n=21 cells). 3) Immature/no SE: BrdU-labeled, GFP expressing cells from animals treated with BrdU five weeks earlier (n=10 cells). 4) Immature+SE: Cells from animals treated with BrdU one week before pilocarpine SE, and killed four weeks after SE (n=19). Previous studies have demonstrated that immature granule cells (<1-2 weeks old) exposed to status epilepticus develop dendritic abnormalities (Jessberger et al., 2007; Walter et al., 2007; Kron et al., 2010) and exhibit reductions in spine density and number (Murphy et al., 2011). Since these studies often utilized different species, models and time points, however, groups three and four were included to confirm that these young cells exhibit similar behavior under the present conditions. Groups are shown schematically in figure 2.

Mature dentate granule cells exposed to status epilepticus

Dendritic structure

Granule cells in the mature+SE group had qualitatively normal apical dendritic trees (Fig.3), exhibiting typical fan-like spreading with dendritic branches terminating at the hippocampal fissure (Claiborne et al., 1990). The apical dendrites of these cells were indistinguishable from age-matched mature/no SE granule cells. Basal dendrites were absent among mature/ no SE cells, and were largely absent among mature+SE cells, although 11.1% of this latter group (2 of 18) possessed large basal dendrites (152 and 153 microns in length) projecting into the hilus. This difference, however, was not significant (p=0.467, z-test), and could be within the normal range, since granule cells from control animals do occasionally possess basal dendrites (Walter et al., 2007).

To generate more quantitative measures of dendritic structure, digital reconstructions were made of mature/no SE and mature+SE granule cells. Standard measures of dendritic structure were similar between groups (Table 1). The trajectory of the initial segment of the apical dendrite – measured relative to a line drawn perpendicular to the granule cell body layer – was also equivalent among groups (mature/no SE, 14.8° [0-33]; mature+SE, 14.2° [0-38]; p=0.962, Mann-Whitney rank sum test [RST]). Finally, the number of self-crossing dendritic branches – a measure used to assess the degree to which dendritic branches occupy overlapping space in the molecular layer – did not differ between mature/no SE and mature +SE cells (Table 1). Self-crossing dendrites were assessed from a two-dimensional perspective.

Dendritic spine changes

Mature+SE granule cells showed consistent reductions in spine density across all three subregions of the dentate molecular layer relative to mature/no SE cells (Figs.4 & 5; IML, p=0.006; MML, p=0.004; OML, p=0.044; RST). Since the dendritic trees for these cells were also reconstructed, it was possible to calculate spine numbers for each molecular layer

subregion and for entire cells (spine density × dendrite length). Spine number was significantly reduced for mature+SE cells in the inner and middle molecular layers relative to mature/no SE cells (Fig.4; IML, p=0.018; MML, p=0.009; RST). No significant difference was evident between groups in the outer molecular layer (Fig.4), spine density reductions in this region being offset by slightly greater dendrite length for mature+SE cells (Table 1). Total spine number (all regions combined) for mature+SE cells, however, was still reduced significantly relative to mature/no SE cells (p=0.040, RST).

Groups were also assessed to determine whether a correlation existed between soma area and spine density. Previous studies, examining 12-week-old cells born one week before status epilepticus, found a positive association among these features (Murphy et al., 2011). Interestingly, spine density was significantly correlated with soma area in the inner (R= 0.600, p=0.011; Pearson Product Moment [PPM] Correlation), middle (R=0.780, p<0.0002; PPM Correlation) and outer (R=0.498, p=0.0498; PPM Correlation) molecular layers for mature+SE cells. By contrast, no significant correlations were found for mature/no SE cells (inner, R= 0.120, p=0.635; middle, R=0.328, p=0.183; outer, R=0.360, p=0.142; PPM correlation).

Immature dentate granule cells exposed to status epilepticus

To ensure that the conditions used for the present study were sufficient to induce dendritic abnormalities, immature granule cells exposed to status epilepticus at one week of age were examined one month after the insult. Since status-exposed immature cells have been examined elsewhere (Murphy et al., 2011), only limited analyses of dendritic structure and spine density were conducted here.

Dendritic structure

Consistent with previous studies (Arisi and Garcia-Cairasco, 2007; Shapiro et al., 2007; Murphy et al., 2011), qualitative examination of apical dendrite morphology revealed gross structural abnormalities among a subset of immature cells exposed to status relative to age-matched control cells (Fig.6). Specifically, while all immature/no SE cells were qualitatively normal, 30% of immature+SE granule cells failed to develop the spreading, fanlike dendritic trees typical of this cell type, instead exhibiting disorganized dendritic trees (3 of 19); collapsed dendritic trees with overlapping, rather than spreading dendrites (2 of 19; Fig.6, A); and dendrites that projected obliquely rather than directly into the molecular layer (1 of 19; Fig.6, B). Collapsed dendritic trees and oblique dendrites correspond to the "closed parasol" and "windblown" deformations (Scheibel and Scheibel, 1973) described previously among 12-week-old cells exposed to status when they were one week-of-age (Murphy et al., 2011). Also consistent with prior work (Jessberger et al., 2007; Walter et al., 2007), 37% of immature+SE cells possessed basal dendrites projecting into the hilus, while basal dendrites were absent among immature/no SE cells (p=0.034; Mann-Whitney rank sum test).

Dendritic spine changes

Dendritic spine density was significantly reduced along dendritic segments located in the inner, middle and outer molecular layers for immature+SE cells relative to immature/no SE cells (Fig.7 and 8; IML, p<0.001; MML, p<0.005; OML, p=0.033; two way ANOVA). Notably, animals treated with pilocarpine or saline at three months of age had significantly lower spine densities in the inner molecular layer relative to animals treated at one month of age, regardless of treatment group. The change is indicative of an age-related reduction in spine density in this region. Similar patterns were evident in the middle and outer molecular layers, although the effects were not significant. No interactions between age and treatment

were found, indicating that the effects of status on spine density were similar at one and three months.

Discussion

In the adult brain, the dentate gyrus contains a mix of mature and immature cells, ranging in age from days to months to years. When challenged by brain injury, these differences in age become important, modulating whether and how the cell responds. In the present study, two-month-old granule cells were exposed to status epilepticus and their structure was examined one month later. At two months of age, granule cells are functionally mature, and have passed the critical period during which new granule cells exhibit enhanced LTP by about two weeks (Ge et al., 2007). Two-month-old granule cells were resistant to developing the gross structural abnormalities evident among younger cells exposed to status, and their dendritic trees were quantitatively similar to age-matched cells from control animals. Intriguingly, however, mature cells exposed to status did exhibit significant reductions in dendritic spine density and number, similar to reductions observed among younger cells (Fig.7). Reductions in spine density were present in all three lamina, and reductions in spine number were evident in the inner and middle molecular layers. These latter changes suggest reduced commissural/associational input and reduced input from medial entorhinal cortex, respectively. Together, these findings demonstrate that while mature granule cells are resistant to seizure-induced changes, they are not immune and can undergo significant restructuring.

Age-dependent plasticity of granule cells in epilepsy

In the present study, two-month-old granule cells exposed to status epilepticus were found to be resistant to developing the abnormal apical dendritic trees evident among younger cells exposed to status (Murphy et al., 2011). The degree of granule cell pathology, however, can vary considerably among epilepsy models, animal strains and protocol conditions. To confirm that the methodology used here was sufficient to induce granule cell dendritic abnormalities, a group of cells birthdated one week before status epilepticus was examined one month after status. These animals were littermates to animals used to study mature granule cells, and the younger cells in these animals readily developed the apical dendrite abnormalities described by our laboratory previously (Murphy et al., 2011), albeit at an earlier timepoint (one month post SE here instead of three months). These findings confirm that the conditions used were capable of producing granule cell pathology, and strongly support the conclusion that the lack of apical dendrite abnormalities among mature cells reflects actual differences in their inherent plasticity.

One week after cell birth, granule cell apical dendritic trees are still very immature and are actively growing, as evidenced by the presence of growth cones at the dendritic tips (Jones et al., 2003; Overstreet-Wadiche and Westbrook, 2006). It seems likely that status epilepticus disrupts this growth, leading to the abnormal dendritic trees shown in figure 6. Consistent with this interpretation, studies of granule cell morphology using the early neuronal marker doublecortin reveal rapid changes in dendritic structure following seizures (Arisi and Garcia-Cairasco, 2007; Shapiro et al., 2007). By contrast, the apical dendritic trees of two-month-old granule cells are structurally mature and lack growth cones, although subtle changes in dendritic structure may continue for several months after birth (Zhao et al., 2006). The overall structure of the dendritic tree, therefore, would appear to relatively fixed, at least for the conditions examined here. Dendritic spines, on the other hand, have long been known to be extremely plastic even among mature neurons, and mature granule cells do not appear to differ in this regard.

Although the mechanism underlying the distorted growth of immature granule cells in epilepsy is unknown, disruption of reelin signaling may play an important role. Reelin is synthesized by Cajal-Retzius cells located in the outer molecular layer of the dentate gyrus. Granule cells in reeler mutant mice, which lack reelin expression, exhibit dendritic anomalies similar to those observed among immature granule cells exposed to status epilepticus (Stanfield and Cowan, 1979; Drakew et al., 2002; Förster et al., 2006). Altered reelin signaling in epilepsy (Gong et al., 2007; Fournier et al., 2010; Haas and Frotscher, 2010; Tinnes et al., 2011; Jaako et al., 2011) may disrupt dendritic growth and orientation, impairing young cells while leaving cells already mature at the time of the insult comparatively unaffected.

Significance of reduced spine density among mature and immature granule cells exposed to status epilepticus

Dendritic spines are the postsynaptic specializations characteristic of excitatory synapses in the CNS. Spine counts, therefore, provide an indirect measure of excitatory synapse number. Direct measures of synapse number by electron microscopy support the utility of spine counts to assess synaptic input. For example, Cardoso and colleagues (2008) found reduced synapse density in the dentate inner and outer molecular layer following electroconvulsive seizures in rats, consistent with the present findings. Nonetheless, not all spines possess functional synapses, and not all excitatory synapses are at spines (for review see Sorra and Harris, 2000; Fiala et al., 2002). The present data, therefore, should be viewed with this caveat in mind.

Although most earlier studies did not assess granule cell age, a pattern of initial spine loss (Isokawa, 1998; Isokawa, 2000; Kurz et al., 2008; Thind et al., 2010) followed by a recovery in spine density (Isokawa, 1998; Isokawa, 2000; Thind et al., 2010) has been observed repeatedly in animal models of epilepsy. Rapid spine loss – prior to the onset of spontaneous seizures in status epilepticus models of epilepsy – implies that status itself is sufficient to induce the change. For the present study, however, we note that spontaneous seizures typically begin within a few weeks after status epilepticus in the pilocarpine model (Shibley and Smith, 2002; Borges et al., 2003; Goffin et al., 2007), so the possibility that the present findings reflect the impact of these seizures in addition to status should not be excluded. Interestingly, a recent study by Wood and colleagues (2011) does provide some insight into this question. They examined the morphology of newborn granule cells exposed to stimulus-evoked seizures in the kindling model of epilepsy, and found no change in spine density among cells exposed to 12-16 seizures. This finding suggests that seizures alone may not account for the reduction in spine density observed here, and that the period of status epilepticus is required. Alternatively, it is also possible that the consequences of spontaneous seizures in the pilocarpine model are distinct from evoked seizures in the kindling model. Future studies might be able to distinguish among these possibilities by controlling spontaneous seizures with anticonvulsive agents.

Status epilepticus results in loss of mossy cells in the dentate hilus (Borges et al., 2003; Boulland et al., 2007; Jiao and Nadler, 2007) and principal cells in entorhinal cortex (Kumar and Buckmaster, 2006; Castro et al., 2011). These neurons target granule cell dendrites in the molecular layer, so rapid spine loss may reflect deafferentation. Excitotoxic injury (Swann et al., 2000) and/or homeostatic mechanisms (Kempermann, 2006) may also play a role. Consistent with the latter possibility, Jakubs and colleagues (2006) found that granule cells born one week after electrically-induced status epilepticus and examined 4-6 weeks later using patch-clamp electrodes exhibited significant reductions in excitatory post-synaptic current (EPSC) frequency. This time course closely matches that of the present study, and the reduction in EPSC frequency is consistent with the reduction in spine density observed here among immature+SE cells. Jakubs and colleagues observed normal EPSC

frequency among mature cells exposed to status. This is in contrast to what the reduction in spine density for mature+SE cells observed here would predict, although since very different methods were used to identify mature cells (BrdU birthdating vs. membrane rise time constant) it is not clear these reflect the same populations. Differences between epilepsy models and species (mouse vs. rat) could also be important. Nonetheless, our findings suggest that pilocarpine-status epilepticus and/or the occurrence of spontaneous seizures lead to a widespread reduction in afferent contacts to immature and mature populations of granule cells one month after the insult.

Physiological studies will be required to elucidate how changes in spine number alter brain function. Notably, a reduction in the number of synaptic inputs does not necessarily imply reduced excitability. Changes in network dynamics, afferent activity patterns, intrinsic neuronal properties and synaptic strength are likely to be important as well. Indeed, work by Kobayashi and colleagues (2003) demonstrated an increase in spontaneous field potentials in the dentate five days after pilocarpine status epilepticus in rats, a time point when widespread spine loss has been observed in other studies (Isokawa, 1998; Isokawa, 2000; Kurz et al., 2008; Thind et al., 2010). The finding suggests that even if spine loss acts to maintain homeostasis, the adaption is not sufficient to preserve normal activity patterns. Finally, the source of afferent input to remaining spines is clearly altered in epileptic animals – at least in the inner molecular layer – where normal commissural/associational inputs are replaced by recurrent excitatory connections with other granule cells (Nadler, 2003; Murphy et al., 2011). The overall reduction in spine numbers observed here, therefore, masks the fact that many of these remaining spines reflect *de novo* recurrent excitatory inputs.

In summary, the present study confirms previous findings that adult-generated granule cells are responsible for the most pronounced neuroplastic changes associated with epilepsy. Importantly, while newborn cells exhibited the most striking changes, mature cells were also affected, exhibiting significant reductions in spine density in all three lamina of the dentate molecular layer and overall reductions in spine number. These findings indicate that both mature and immature granule cells may contribute in significant ways to epileptogenesis and to comorbidities associated with the disease.

Acknowledgments

Literature Cited

Altman J, Das GD. Autoradiographic and histological evidence of postnatal hippocampal neurogenesis in rats. J Comp Neurol. 1965; 124(3):319–35. [PubMed: 5861717]

Arida RM, de Jesus Vieira A, Cavalheiro EA. Effect of physical exercise on kindling development. Epilepsy Res. 1998 Apr; 30(2):127–32. [PubMed: 9600544]

Arisi GM, Garcia-Cairasco N. Doublecortin-positive newly born granule cells of hippocampus have abnormal apical dendritic morphology in the pilocarpine model of temporal lobe epilepsy. Brain Res. 2007 Aug 24.1165:126–34. [PubMed: 17662262]

Borges K, Gearing M, McDermott DL, Smith AB, Almonte AG, Wainer BH, Dingledine R. Neuronal and glial pathological changes during epileptogenesis in the mouse pilocarpine model. Exp Neurol. 2003; 182(1):21–34. [PubMed: 12821374]

Boulland JL, Ferhat L, Tallak Solbu T, Ferrand N, Chaudhry FA, Storm-Mathisen J, Esclapez M. Changes in vesicular transporters for gamma-aminobutyric acid and glutamate reveal vulnerability

and reorganization of hippocampal neurons following pilocarpine-induced seizures. J Comp Neurol. 2007; 503(3):466–85. [PubMed: 17503488]

Bundman MC, Pico RM, Gall CM. Ultrastructural plasticity of the dentate gyrus granule cells following recurrent limbic seizures: I. Increase in somatic spines. Hippocampus. 1994; 4(5):601–10. [PubMed: 7889130]

Cameron MC, Zhan RZ, Nadler JV. Morphologic integration of hilar ectopic granule cells into dentate gyrus circuitry in the pilocarpine model of temporal lobe epilepsy. J Comp Neurol. 2011 in press.

Cardoso A, Assunção M, Andrade JP, Pereira PA, Madeira MD, Paula-Barbosa MM, Lukoyanov NV. Loss of synapses in the entorhinal-dentate gyrus pathway following repeated induction of electroshock seizures in the rat. J Neurosci Res. 2008; 86(1):71–83. [PubMed: 17705293]

Castro OW, Furtado MA, Tilelli CQ, Fernandes A, Pajolla GP, Garcia-Cairasco N. Comparative neuroanatomical and temporal characterization of FluoroJade-positive neurodegeneration after status epilepticus induced by systemic and intrahippocampal pilocarpine in Wistar rats. Brain Res. 2011; 1374:43–55. [PubMed: 21147076]

Claiborne BJ, Amaral DG, Cowan WM. Quantitative, three-dimensional analysis of granule cell dendrites in the rat dentate gyrus. J Comp Neurol. 1990; 302(2):206–19. [PubMed: 2289972]

da Silva AV, Houzel JC, Targas Yacubian EM, Carrete H Jr, Sakamoto AC, Priel MR, Martins HH, Oliveira I, Garzon E, Stavale JN, da Silva Centeno R, Machado H, Cavalheiro EA. Dysmorphic neurons in patients with temporal lobe epilepsy. Brain Res. 2006; 1072:200–207. [PubMed: 16430872]

Danzer SC, Pan E, Nef S, Parada LF, McNamara JO. Altered Regulation of BDNF Protein in Hippocampus Following Slice Preparation. Neuroscience. 2004; 126(4):859–69. [PubMed: 15207321]

Danzer SC. Depression, stress, epilepsy and adult neurogenesis. Exp Neurol. 201110.1016/j.expneurol. 2011.05.023

Deller T, Drakew A, Frotscher M. Different primary target cells are important for fiber lamination in the fascia dentata: a lesson from reeler mutant mice. Exp Neurol. 1999; 156(2):239–53. [PubMed: 10328933]

Deng W, Aimone JB, Gage FH. New neurons and new memories: how does adult hippocampal neurogenesis affect learning and memory? Nat Rev Neurosci. 2010; 11(5):339–50. [PubMed: 20354534]

Drakew A, Deller T, Heimrich B, Gebhardt C, Del Turco D, Tielsch A, Förster E, Herz J, Frotscher M. Dentate granule cells in reeler mutants and VLDLR and ApoER2 knockout mice. Exp Neurol. 2002; 176(1):12–24. [PubMed: 12093079]

Eriksson PS, Perfilieva E, Bjork-Eriksson T, Alborn AM, Nordborg C, Peterson DA, Gage FH. Neurogenesis in the adult human hippocampus. Nat Med. 1998; 4(11):1313–7. [PubMed: 9809557]

Feng G, Mellor RH, Bernstein M, Keller-Peck C, Nguyen QT, Wallace M, Nerbonne JM, Lichtman JW, Sanes JR. Imaging neuronal subsets in transgenic mice expressing multiple spectral variants of GFP. Neuron. 2000; 28(1):41–51. [PubMed: 11086982]

Fiala JC, Spacek J, Harris KM. Dendritic spine pathology: cause or consequence of neurological disorders? Brain Res Brain Res Rev. 2002; 39(1):29–54. [PubMed: 12086707]

Förster E, Jossin Y, Zhao S, Chai X, Frotscher M, Goffinet AM. Recent progress in understanding the role of Reelin in radial neuronal migration, with specific emphasis on the dentate gyrus. Eur J Neurosci. 2006; 23(4):901–9. [PubMed: 16519655]

Fournier NM, Andersen DR, Botterill JJ, Sterner EY, Lussier AL, Caruncho HJ, Kalynchuk LE. The effect of amygdala kindling on hippocampal neurogenesis coincides with decreased reelin and DISC1 expression in the adult dentate gyrus. Hippocampus. 2010; 20(5):659–71. [PubMed: 19499587]

Ge S, Yang CH, Hsu KS, Ming GL, Song H. A critical period for enhanced synaptic plasticity in newly generated neurons of the adult brain. Neuron. 2007; 54(4):559–66. [PubMed: 17521569]

Geinisman Y, Morrell F, deToledo-Morrell L. Remodeling of synaptic architecture during hippocampal "kindling". Proc Natl Acad Sci U S A. 1988; 85(9):3260–4. [PubMed: 2834740]

Goffin K, Nissinen J, Van Laere K, Pitkänen A. Cyclicity of spontaneous recurrent seizures in pilocarpine model of temporal lobe epilepsy in rat. Exp Neurol. 2007; 205(2):501–5. [PubMed: 17442304]

Gong C, Wang TW, Huang HS, Parent JM. Reelin regulates neuronal progenitor migration in intact and epileptic hippocampus. J Neurosci. 2007; 27(8):1803–11. [PubMed: 17314278]

Haas CA, Frotscher M. Reelin deficiency causes granule cell dispersion in epilepsy. Exp Brain Res. 2010; 200(2):141–9. [PubMed: 19633980]

Houser CR. Granule cell dispersion in the dentate gyrus of humans with temporal lobe epilepsy. Brain Res. 1990; 535(2):195–204. [PubMed: 1705855]

Isokawa M. Remodeling dendritic spines in the rat pilocarpine model of temporal lobe epilepsy. Neurosci Lett. 1998; 258(2):73–6. [PubMed: 9875530]

Isokawa M. Remodeling dendritic spines of dentate granule cells in temporal lobe epilepsy patients and the rat pilocarpine model. Epilepsia. 2000; 41 6:S14–7. [PubMed: 10999513]

Jaako K, Aonurm-Helm A, Kalda A, Anier K, Zharkovsky T, Shastin D, Zharkovsky A. Repeated citalopram administration counteracts kainic acid-induced spreading of PSA-NCAM-immunoreactive cells and loss of reelin in the adult mouse hippocampus. Eur J Pharmacol. 2011; 666(1-3):61–71. [PubMed: 21596030]

Jakubs K, Nanobashvili A, Bonde S, Ekdahl CT, Kokaia Z, Kokaia M, Lindvall O. Environment Matters: Synaptic Properties of Neurons Born in the Epileptic Adult Brain Develop to Reduce Excitability. Neuron. 2006; 52(6):1047–1059. [PubMed: 17178407]

Jessberger S, Zhao C, Toni N, Clemenson GD Jr, Li Y, Gage FH. Seizure-associated, aberrant neurogenesis in adult rats characterized with retrovirus-mediated cell labeling. J Neurosci. 2007; 27(35):9400–7. [PubMed: 17728453]

Jiao Y, Nadler JV. Stereological analysis of GluR2-immunoreactive hilar neurons in the pilocarpine model of temporal lobe epilepsy: correlation of cell loss with mossy fiber sprouting. Exp Neurol. 2007; 205(2):569–82. [PubMed: 17475251]

Jones SP, Rahimi O, O'Boyle MP, Diaz DL, Claiborne BJ. Maturation of granule cell dendrites after mossy fiber arrival in hippocampal field CA3. Hippocampus. 2003; 13(3):413–27. [PubMed: 12722981]

Kaplan MS, Hinds JW. Neurogenesis in the adult rat: electron microscopic analysis of light radioautographs. Science. 1977; 197(4308):1092–4. [PubMed: 887941]

Kempermann G. They are not too excited: the possible role of adult-born neurons in epilepsy. Neuron. 2006 Dec 21; 52(6):935–7. [PubMed: 17178397]

Kron MM, Zhang H, Parent JM. The developmental stage of dentate granule cells dictates their contribution to seizure-induced plasticity. J Neurosci. 2010; 30(6):2051–9. [PubMed: 20147533]

Kumar SS, Buckmaster PS. Hyperexcitability, interneurons, and loss of GABAergic synapses in entorhinal cortex in a model of temporal lobe epilepsy. J Neurosci. 2006; 26(17):4613–23. [PubMed: 16641241]

Kurz JE, Moore BJ, Henderson SC, Campbell JN, Churn SB. A cellular mechanism for dendritic spine loss in the pilocarpine model of status epilepticus. Epilepsia. 2008 Oct; 49(10):1696–710. [PubMed: 18479390]

Mathews EA, Morgenstern NA, Piatti VC, Zhao C, Jessberger S, Schinder AF, Gage FH. A distinctive layering pattern of mouse dentate granule cells is generated by developmental and adult neurogenesis. J Comp Neurol. 2010; 518(22):4479–90. [PubMed: 20886617]

Murphy BL, Danzer SC. Somatic translocation: a novel mechanism of granule cell dendritic dysmorphogenesis and dispersion. J Neurosci. 2011; 31(8):2959–64. [PubMed: 21414917]

Murphy BL, Pun RYK, Yin H, Loepke AW, Danzer SC. Heterogeneous integration of adult-generated granule exposed to status epilepticus. Journal of Neuroscience. 2011; 31(1):105–17. [PubMed: 21209195]

Nadler JV. The recurrent mossy fiber pathway of the epileptic brain. Neurochem Res. 2003; 28(11):1649–58. [PubMed: 14584819]

Overstreet-Wadiche LS, Westbrook GL. Functional maturation of adult-generated granule cells. Hippocampus. 2006; 16(3):208–15. [PubMed: 16411232]

Parent JM, Yu TW, Leibowitz RT, Geschwind DH, Sloviter RS, Lowenstein DH. Dentate granule cell neurogenesis is increased by seizures and contributes to aberrant network reorganization in the adult rat hippocampus. J Neurosci. 1997; 17(10):3727–38. [PubMed: 9133393]

Parent JM, Elliott RC, Pleasure SJ, Barbaro NM, Lowenstein DH. Aberrant seizure-induced neurogenesis in experimental temporal lobe epilepsy. Ann Neurol. 2006; 59(1):81–91. [PubMed: 16261566]

Parent JM, Murphy GG. Mechanisms and functional significance of aberrant seizure-induced hippocampal neurogenesis. Epilepsia. 2008; 49 5:19–25. [PubMed: 18522597]

Paxinos, G.; Franklin, KB. The Mouse Brain in Stereotaxic Coordinates. Academic Press; London: 2001.

Pierce JP, Melton J, Punsoni M, McCloskey DP, Scharfman HE. Mossy fibers are the primary source of afferent input to ectopic granule cells that are born after pilocarpine-induced seizures. Exp Neurol. 2005; 196(2):316–31. [PubMed: 16342370]

Pierce JP, McCloskey DP, Scharfman HE. Morphometry of hilar ectopic granule cells in the rat. J Comp Neurol. 2011 Apr 15; 519(6):1196–218. [PubMed: 21344409]

Ribak CE, Tran PH, Spigelman I, Okazaki MM, Nadler JV. Status epilepticus-induced hilar basal dendrites on rodent granule cells contribute to recurrent excitatory circuitry. J Comp Neurol. 2000; 428(2):240–53. [PubMed: 11064364]

Scharfman HE, Goodman JH, Sollas AL. Granule-like neurons at the hilar/CA3 border after status epilepticus and their synchrony with area CA3 pyramidal cells: functional implications of seizure-induced neurogenesis. J Neurosci. 2000; 20(16):6144–58. [PubMed: 10934264]

Scheibel, ME.; Scheibel, AB. Hippocampal pathology in temporal lobe epilepsy: A golgi survey. In: Brazier, MAB., editor. Epilepsy: Its phenomena in man. New York: Raven Press; 1973. p. 311-37.

Shapiro LA, Ribak CE. Newly born dentate granule neurons after pilocarpine-induced epilepsy have hilar basal dendrites with immature synapses. Epilepsy Res. 2006; 69(1):53–66. [PubMed: 16480853]

Shapiro LA, Figueroa-Aragon S, Ribak CE. Newly generated granule cells show rapid neuroplastic changes in the adult rat dentate gyrus during the first five days following pilocarpine-induced seizures. Eur J Neurosci. 2007; 26(3):583–92. [PubMed: 17686039]

Shibley H, Smith BN. Pilocarpine-induced status epilepticus results in mossy fiber sprouting and spontaneous seizures in C57BL/6 and CD-1 mice. Epilepsy Res. 2002; 49(2):109–20. [PubMed: 12049799]

Sorra KE, Harris KM. Overview on the structure, composition, function, development, and plasticity of hippocampal dendritic spines. Hippocampus. 2000; 10(5):501–11. [PubMed: 11075821]

Stanfield BB, Cowan WM. The morphology of the hippocampus and dentate gyrus in normal and reeler mice. J Comp Neurol. 1979; 185(3):393–422. [PubMed: 438366]

Swann JW, Al-Noori S, Jiang M, Lee CL. Spine loss and other dendritic abnormalities in epilepsy. Hippocampus. 2000; 10(5):617–25. [PubMed: 11075833]

Thind KK, Ribak CE, Buckmaster PS. Synaptic input to dentate granule cell basal dendrites in a rat model of temporal lobe epilepsy. J Comp Neurol. 2008 Jul 10; 509(2):190–202. [PubMed: 18461605]

Thind KK, Yamawaki R, Phanwar I, Zhang G, Wen X, Buckmaster PS. Initial loss but later excess of GABAergic synapses with dentate granule cells in a rat model of temporal lobe epilepsy. J Comp Neurol. 2010 Mar 1; 518(5):647–67. [PubMed: 20034063]

Tinnes S, Schäfer MK, Flubacher A, Münzner G, Frotscher M, Haas CA. Epileptiform activity interferes with proteolytic processing of Reelin required for dentate granule cell positioning. FASEB J. 2011; 25(3):1002–13. [PubMed: 21148112]

van Groen T, Miettinen P, Kadish I. The entorhinal cortex of the mouse: organization of the projection to the hippocampal formation. Hippocampus. 2003; 13(1):133–49. [PubMed: 12625464]

van Praag H, Schinder AF, Christie BR, Toni N, Palmer TD, Gage FH. Functional neurogenesis in the adult hippocampus. Nature. 2002; 415(6875):1030–4. [PubMed: 11875571]

von Campe G, Spencer DD, de Lanerolle NC. Morphology of dentate granule cells in the human epileptogenic hippocampus. Hippocampus. 1997; 7:472–488. [PubMed: 9347345]

Walter C, Murphy BL, Pun RY, Spieles-Engemann AL, Danzer SC. Pilocarpine-induced seizures cause selective time-dependent changes to adult-generated hippocampal dentate granule cells. J Neurosci. 2007; 27(28):7541–52. [PubMed: 17626215]

West MJ, Andersen AH. An allometric study of the area dentata in the rat and mouse. Brain Res. 1980; 2(3):317–48. [PubMed: 7470858]

Wood JC, Jackson JS, Jakubs K, Chapman KZ, Ekdahl CT, Kokaia Z, Kokaia M, Lindvall O. Functional integration of new hippocampal neurons following insults to the adult brain is determined by characteristics of pathological environment. Exp Neurol. 2011; 229(2):484–93. [PubMed: 21459089]

Zhao C, Teng EM, Summers RG Jr, Ming GL, Gage FH. Distinct morphological stages of dentate granule neuron maturation in the adult mouse hippocampus. J Neurosci. 2006; 26(1):3–11. [PubMed: 16399667]

Highlights

- Dentate granule cell plasticity in temporal lobe epilepsy depends on cell age

- Immature granule cells exposed to status epilepticus develop abnormal dendrites

- Mature granule cells exposed to status epileptics exhibit normal apical dendrites

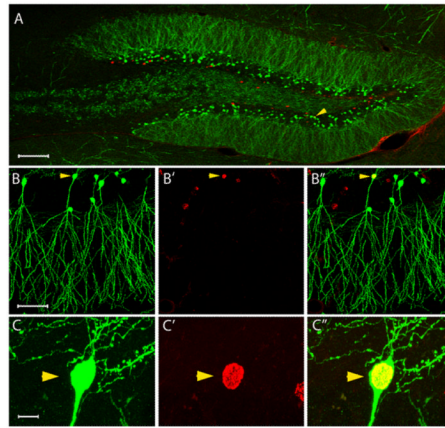- Mature and immature granule cells exhibit reduced spine density after status epilepticus

Figure 1.
A: Panoramic confocal image of the dentate gyrus showing GFP (green) and BrdU (red) labeling. The arrowhead denotes a BrdU-labeled, GFP-expressing granule cell. **B:** Example of a BrdU-labeled, GFP-expressing granule cell. GFP immunostaining (B), BrdU immunostaining (B′) and merged (B″) images are shown. **C:** Higher resolution image of the cell shown in B. GFP immunostaining (C), BrdU immunostaining (C′) and merged (C″) images are shown, with the latter depicting the double-labeled nucleus in yellow. Scale bars = 100 μm (A); 50 μm (B); 10 μm (C).
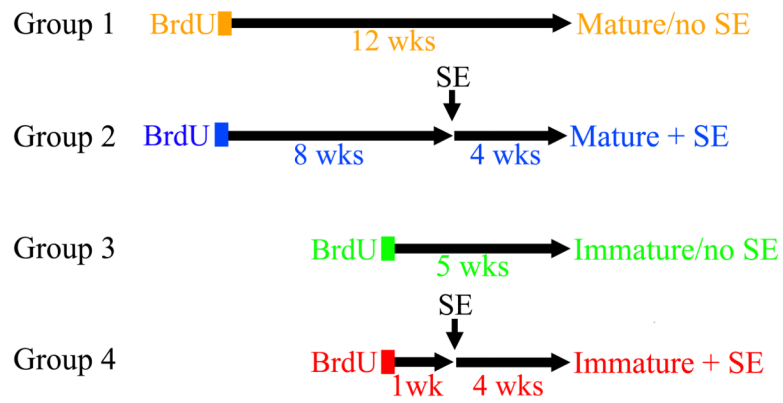
Figure 2.
Schematic outlining the treatment and neuronal birthdating strategy for the four study groups. BrdU was given either eight weeks (groups 1-2) or one week (groups 3-4) prior to pilocarpine treatment to induce status epilepticus (SE) and the later development of epilepsy. Control animals (no SE) received saline. All animals were killed four weeks after pilocarpine or saline treatment.
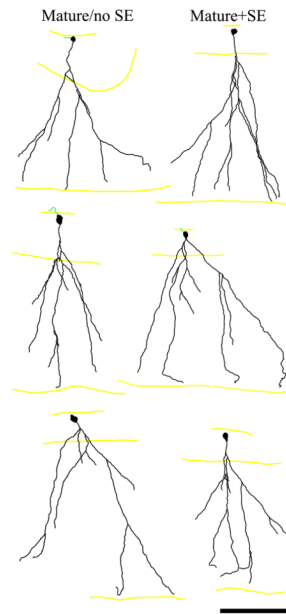
Figure 3.
Neurolucida reconstructions of granule cells exposed to pilocarpine-status epilepticus (mature+SE) when they were eight weeks old. Examination of these cells four weeks later revealed normal apical dendritic structures relative to age-matched cells from control animals (mature/no SE). Apical dendrites are shown in black and axons in green. Yellow lines denote the granule cell layer – hilar border, the granule cell layer – molecular layer border and the hippocampal fissure, from top to bottom respectively. Scale bar = 100 μm.
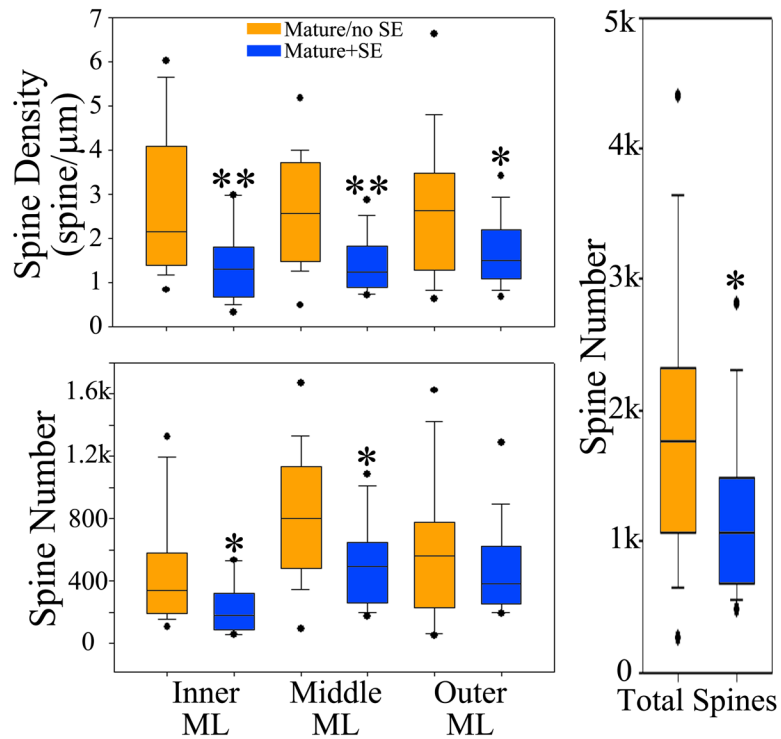
Figure 4.
Box plots of spine density and number. Boxes reflect the 25th and 75th percentiles with the median line shown. Whiskers show the 5th and 95th percentiles, and dots indicate each outlier. **Top panel:** Spine density along granule cell dendrites located in the inner, middle and outer molecular layers (ML) was significantly reduced among mature+SE cells (blue) relative to mature/no SE cells (orange). Spine number was similarly reduced in the inner and middle molecular layers (**bottom panel**), and significant reductions in total spine number (all three regions combined) were evident (**right panel**), *p<0.05, **, p<0.01, Mann-Whitney rank sum test.
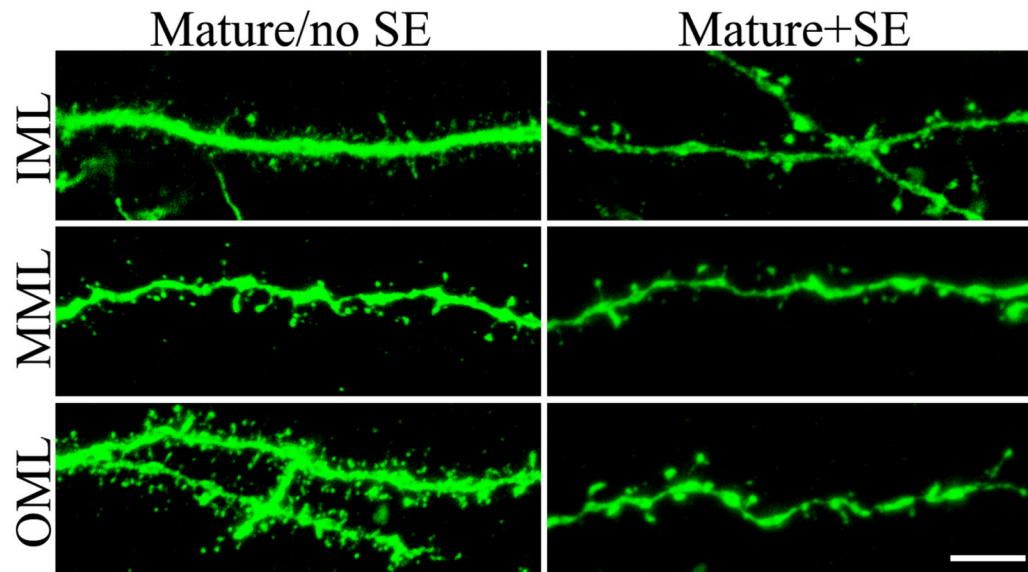
Figure 5.
Confocal reconstructions of dendritic segments from BrdU-labeled, GFP-expressing mature granule cells exposed to saline (mature/no SE) or status epilepticus (mature+SE). Segments from the inner (IML), middle (MML) and outer (OML) molecular layers are shown. Reduced spine density is evident in all three layers among mature+SE cells relative to controls. Scale bar = 5 μm.
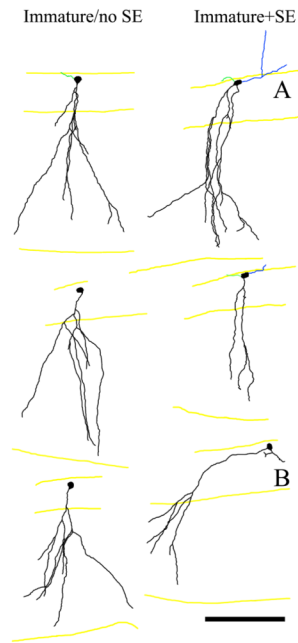
Figure 6.
Neurolucida reconstructions of granule cells exposed to pilocarpine-status epilepticus (immature+SE) when they were one week old and examined four weeks later. Analysis revealed distorted apical dendritic trees among a subset relative to age-matched cells from control animals (immature/no SE). Cells with collapsed (A) and windswept (B) dendritic trees are shown. Apical dendrites are shown in black, axons in green and basal dendrites in blue. Yellow lines denote the granule cell layer – hilar border, the granule cell layer – molecular layer border and the hippocampal fissure, from top to bottom respectively. Scale bar = 100 μm.
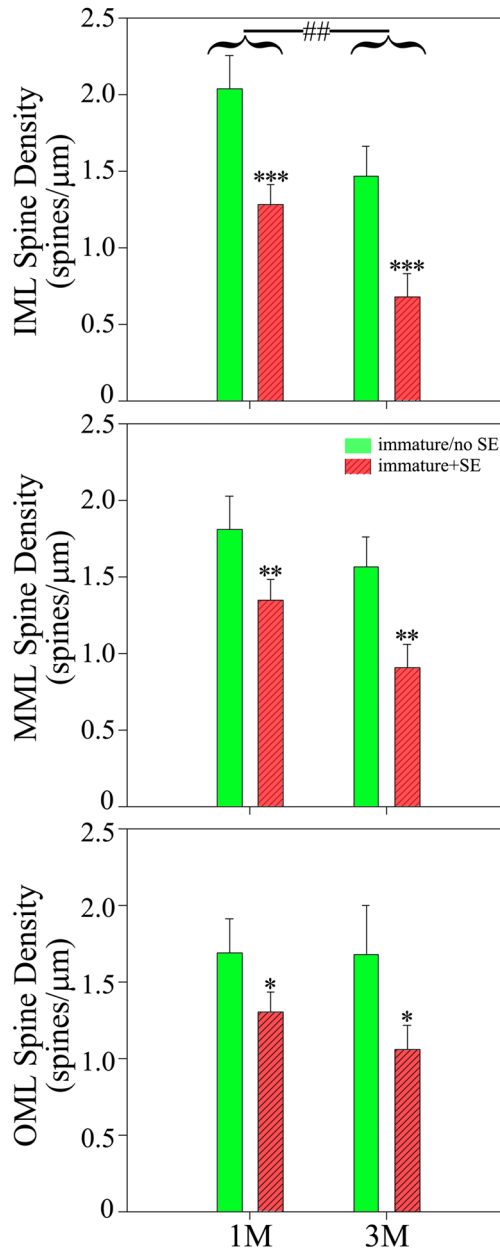
Figure 7.
Spine density along granule cell dendrites located in the inner, middle and outer molecular layers (ML) was significantly reduced among immature+SE cells (red) relative to immature/no SE cells (green). For clarity, data are presented with groups broken down by treatment (status epilepticus [SE] or no SE) and mouse age at which treatments were begun (one month [1M] or three months [3M]), although statistical comparisons were made using a two-way ANOVA controlling for the two variables. Spine density was significantly reduced following status epilepticus; *, **, ***, p<0.05, p<0.01 and p<0.001, respectively. Within the inner molecular layer, spine density was also significantly lower for 1M animals vs. 3M animals, regardless of treatment group; ##, p<0.01. Values are least square means.
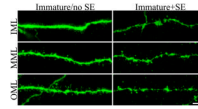
Figure 8.
Confocal reconstructions of dendritic segments from BrdU-labeled, GFP-expressing immature granule cells exposed to saline (immature/no SE) or status epilepticus (immature +SE). Segments from the inner (IML), middle (MML) and outer (OML) molecular layers are shown. Note the reduction in spine density among immature+SE segments relative to controls. Scale bar = 5 μm.

Table 1

	# cells	BD Length (μm)	Soma area (μm²)	% cells with 2 AD's [median (range)]	AD Branch Points	Self-crossing AD's	Terminal branch order of natural endings	AD Length				
								DGCL layer	IML	MML	OML	Total
Mature/no	18	0.0	63.0±	11.1%	6.3±	3.0	4.6 (3-8)	74.2	139.3	315.4	204.5	786.0
SE		(0-0)	3.7	[1(1-2)]	0.4	(0-7)		(18-121)	(93-226)	(96-525)	(79-353)	(432-956)
Mature	21	0.0	58.1±	14.3%	6.2±	3.0	4.0 (1-6)	69.9	158.8	330.9	233.2	799.6
+SE		(0-153)	3.7	[1(1-2)]	0.5	(0-8)		(10-144)	(105-308)	(215-555)	(38-581)	(553-1290)

Values are means ± SEM or medians (range).